Thermal-neutron capture by ^{208}Pb

J. C. Blackmon and S. Raman
Physics Division, Oak Ridge National Laboratory, Oak Ridge, Tennessee 37831

J. K. Dickens
Joint Institute for Heavy Ion Research, Oak Ridge, Tennessee 37831
and Department of Physics and Astronomy, University of Tennessee, Knoxville, Tennessee 37996

R. M. Lindstrom and R. L. Paul
Analytical Chemistry Division, National Institute of Standards and Technology, Gaithersburg, Maryland 20899

J. E. Lynn
Los Alamos National Laboratory, Los Alamos, New Mexico 87545
(Received 8 November 2001; published 12 March 2002)

We have observed seven γ rays following subthermal-neutron capture by ^{208}Pb and incorporated them into a level scheme of ^{209}Pb consisting of five excited levels. The measured neutron separation energy of ^{209}Pb is 3938.0 ± 0.5 keV. The thermal-neutron capture cross section of ^{208}Pb was determined to be 230 ± 12 μb. The theoretical estimates are 860 μb or 550 μb, depending on the model used for the compound-nuclear component; however, these values are not inconsistent with the data if the statistical distribution of the theoretical estimates is taken into account. The thermal-neutron capture cross sections for ^{206}Pb and ^{207}Pb were also determined and found to be 26.6 ± 1.2 mb and 610 ± 30 mb, respectively.

DOI: 10.1103/PhysRevC.65.045801 PACS number(s): 25.40.Lw, 26.20.+f, 27.80.+w

I. INTRODUCTION

The doubly magic nucleus ^{208}Pb has one of the smallest cross sections for neutron capture of any stable nucleus [1]. The value $Q=3.94$ MeV for the ^{208}Pb$(n,\gamma)^{209}$Pb reaction is the lowest (n,γ) Q value for any stable nucleus heavier than ^{15}N [2]. The low density of states in ^{209}Pb near the neutron threshold means that few resonances exist in the ^{208}Pb$(n,\gamma)^{209}$Pb reaction at low neutron energies [3], and the direct-capture process [4] is expected to dominate the capture cross section. While the direct-capture process is well known in light nuclei [5–12], there have been few studies in heavier systems. The ^{208}Pb isotope is a good target for the study of direct capture, but few measurements have been performed, and the nature of the ^{208}Pb$(n,\gamma)^{209}$Pb cross section for $E_n<30$ keV remains largely unknown.

The ^{208}Pb$(n,\gamma)^{209}$Pb cross section is also important for understanding the nucleosynthesis of the heavy elements. The lead isotopes are produced by slow-neutron capture (s-process) nucleosynthesis [13]. The heaviest element that can be produced by the s process is ^{209}Bi. This isotope may be produced only weakly by the s process and instead result primarily from the alpha decays of heavier nuclei produced by rapid-neutron capture (r-process) nucleosynthesis [14]. The abundance of ^{209}Bi could provide an important constraint on the neutron flux in the s process [15,16]. The origin of ^{209}Bi remains uncertain resulting from uncertainties in the ^{208}Pb$(n,\gamma)^{209}$Pb cross section.

The resonant ^{208}Pb$(n,\gamma)^{209}$Pb cross section has been studied by both neutron capture and transmission measurements on ^{208}Pb at pulsed neutron sources, and the lowest-energy resonance was reported at $E_n=43.3$ keV [16–18]. A state ($J=\frac{3}{2},\frac{5}{2}$,or $\frac{7}{2}$) seen in the ^{208}Pb$(d,p)^{209}$Pb [19] and ^{207}Pb$(t,p)^{209}$Pb [20] reactions at $E_x=3947\pm5$ keV, which would correspond to a resonance at $E_n\approx9$ keV, has not been observed in neutron capture or transmission measurements. If no significant resonances exist for $E_n<43$ keV, then the direct-capture process will dominate the cross section in this energy region which is important for the s process [16,21].

Only three measurements of the total ^{208}Pb$(n,\gamma)^{209}$Pb cross section have been reported. A value of 6.5 ± 1.0 mb was reported from measurements using a natural lead sample and an Sb-Be photoneutron source ($E_n=24\pm3$ keV) [22]. A measurement was performed more recently at the Karlsruhe 3.75-MV Van de Graaff accelerator using a distribution of neutrons from the ^{7}Li$(p,n)^{7}$Be reaction that was designed to closely approximate that of a Maxwell-Boltzmann distribution with a thermal energy of $kT=25$ keV. A capture cross section of 0.31 ± 0.02 mb was reported [23].

The only reported measurement of the thermal-neutron capture cross section is by Emery. We reprint here the relevant portions of his report [24]: ''Thermal-Neutron Cross Sections. — The center hole in the east D_2O tank of the Bulk Shielding Reactor has a thermal-neutron flux of 1.2×10^{12} neutrons cm^{-2} sec^{-1}. This facility was used to determine the thermal-neutron [capture] cross sections for the ^{64}Ni$(n,\gamma)^{65}$Ni and ^{208}Pb$(n,\gamma)^{209}$Pb reactions. Dilute Au-Al alloy (0.100% Au) was used to measure the thermal-neutron flux . . . . The disintegration rate of ^{209}Pb was determined by a 4π beta counter . . . . The thermal-neutron [capture] cross section of ^{208}Pb was determined to be 487 ± 30 microbarns.'' No further experimental details are reported.

We have measured the ^{208}Pb$(n,\gamma)^{209}$Pb cross section using a cold neutron beam. Our experiment provides the first measurement of high-resolution γ-ray energy spectra produced from this reaction. Cross sections for the

TABLE I. The isotopic composition of the radiogenic lead sample used in these measurements.

Isotope	Atom %
204	<0.04
206	26.0 ± 0.2
207	1.66 ± 0.04
208	72.3 ± 0.2

^{206}Pb$(n,\gamma)^{207}$Pb and ^{207}Pb$(n,\gamma)^{208}$Pb reactions were also measured. At low neutron energies, $E_n<1$ keV, the centrifugal barrier suppresses the interaction of neutrons with angular momentum other than $l=0$. The cross section at these energies is expected to have the usual $1/v$ energy dependence. We deduce thermal-neutron capture cross sections for ^{206}Pb, ^{207}Pb, and ^{208}Pb from our measurements with cold neutrons under this assumption.

The experimental technique is described in Sec. II. The results are presented in Sec. III, and the level scheme of ^{209}Pb deduced from these measurements is discussed in Sec. IV. The cross sections for the ^{206}Pb$(n,\gamma)^{207}$Pb and ^{207}Pb$(n,\gamma)^{208}$Pb reactions are presented in Sec. V. The theory of radiative capture is described briefly in Sec. VI. Using this theory, we have calculated the cross sections for neutron capture to states in ^{209}Pb and have compared them to the measured values. Conclusions and plans for further study are presented in Sec. VII.

II. EXPERIMENT DESCRIPTION

The ^{208}Pb$(n,\gamma)^{209}$Pb reaction was studied at the National Institute for Standards and Technology (NIST) Center for Neutron Research using neutron beams from the Research Reactor NBSR. Measurements were performed using a guided, cold neutron beam extracted from the liquid hydrogen cold source. A radiogenic lead sample with enhanced ^{208}Pb content was placed 41 m from the cold source on the neutron guide NG-7. The neutron beam was filtered through 12.7 mm of beryllium and a 203-mm-thick single-crystal bismuth filter. For neutron energies less than 5.2 meV, the neutron energy distribution was approximately that of a Maxwellian corresponding to a temperature of 20 K (1.7 meV). Neutrons with energies greater than 5.2 meV were greatly attenuated by the filters in the beam, and there are essentially no fast neutrons at the sample position.

The lead sample used in these measurements consisted of 2.318 g (18 mm diameter by 0.8 mm thick) of radiogenic lead. The isotopic composition of the sample was determined by mass spectrometry and is given in Table I. The sample was held under vacuum in a magnesium alloy chamber with thin (0.5-mm-thick) entrance and exit windows. The sample was oriented at 45° relative to the incident neutron beam. The neutron beam was collimated to 20 mm in diameter by a ^{6}Li-glass aperture. The sample was smaller than the neutron beam; therefore, the number of neutron captures was proportional to the total number of target atoms and the neutron fluence rate.

Data were collected using a composite sample consisting of the radiogenic lead with a 0.402-g standard sample of reactor-grade graphite (with the same 18 mm diameter as the lead sample). The cross sections for the production of γ rays from the ^{208}Pb$(n,\gamma)^{209}$Pb reaction were determined by normalizing the observed yields attributed to this reaction to those from the ^{12}C$(n,\gamma)^{13}$C reaction. This normalization procedure eliminates potential sources of systematic uncertainty; for example, as might result from the neutron fluence and absolute detection efficiency. Cross sections determined in this manner depend only upon the yields, the ratio of the number of target atoms, and relative efficiencies for γ-ray detection.

Prompt capture γ rays were detected by the NIST Prompt-Gamma Activation Analysis (PGAA) Spectrometer, a 26% high-purity germanium detector with a surrounding bismuth germanate (BGO) Compton-suppression detector [25,26]. The detector was completely shielded, except for the line-of-sight to the sample, by a 10-cm-thick layer of lead and a layer of ^{6}Li-loaded plastic. A conical lead collimator between the detector and sample restricted the detector's field of view to an area slightly larger than the sample size. The photopeak efficiency of the detector was determined at 46 γ-ray energies between 122 and 8579 keV by measuring the yields of γ rays from a calibrated ^{152}Eu source [27] and from the standard ^{35}Cl$(n,\gamma)^{36}$Cl reaction [28]. For studying the latter reaction, a polyvinyl chloride sample with the same diameter as the lead sample was used.

III. RESULTS

A γ-ray energy spectrum was collected for a period of 69.6 h using the composite sample of radiogenic lead and graphite. A portion of this spectrum is shown in Fig. 1(a). Spectra were also collected using the graphite sample only and with the radiogenic lead sample only. The spectrum taken with the carbon sample is also shown in Fig. 1(a) (with an arbitrary normalization). The spectrum taken with the carbon sample was normalized to the spectrum taken with the composite sample using the yields of the 1262- and 3684-keV γ rays from the ^{12}C$(n,\gamma)^{13}$C reaction, and subtracted to obtain a net spectrum attributed to interaction of the neutron beam with the radiogenic lead sample. A portion of this net spectrum is shown in Fig. 1(c). Seven peaks were observed at energies that correspond to either primary transitions to known levels in ^{209}Pb or secondary transitions between known levels in ^{209}Pb below the neutron threshold. No peaks were observed in the carbon spectrum at these energies, and the peaks assigned to ^{209}Pb could not be associated with any likely background source [29,30].

The energies of the γ rays attributed to the ^{208}Pb$(n,\gamma)^{209}$Pb reaction are summarized in the first column of Table II. The cross sections for the production of these γ rays, I_γ, were determined by normalizing the observed yields, $Y(E_\gamma)$ to that of the 1262-keV γ ray from the ^{12}C$(n,\gamma)^{13}$C reaction by

$$I_\gamma = 4.11 \frac{Y(E_\gamma)}{Y(1262\ \text{keV})} \frac{\epsilon(1262\ \text{keV})}{\epsilon(E_\gamma)} I_{1262}, \qquad (3.1)$$

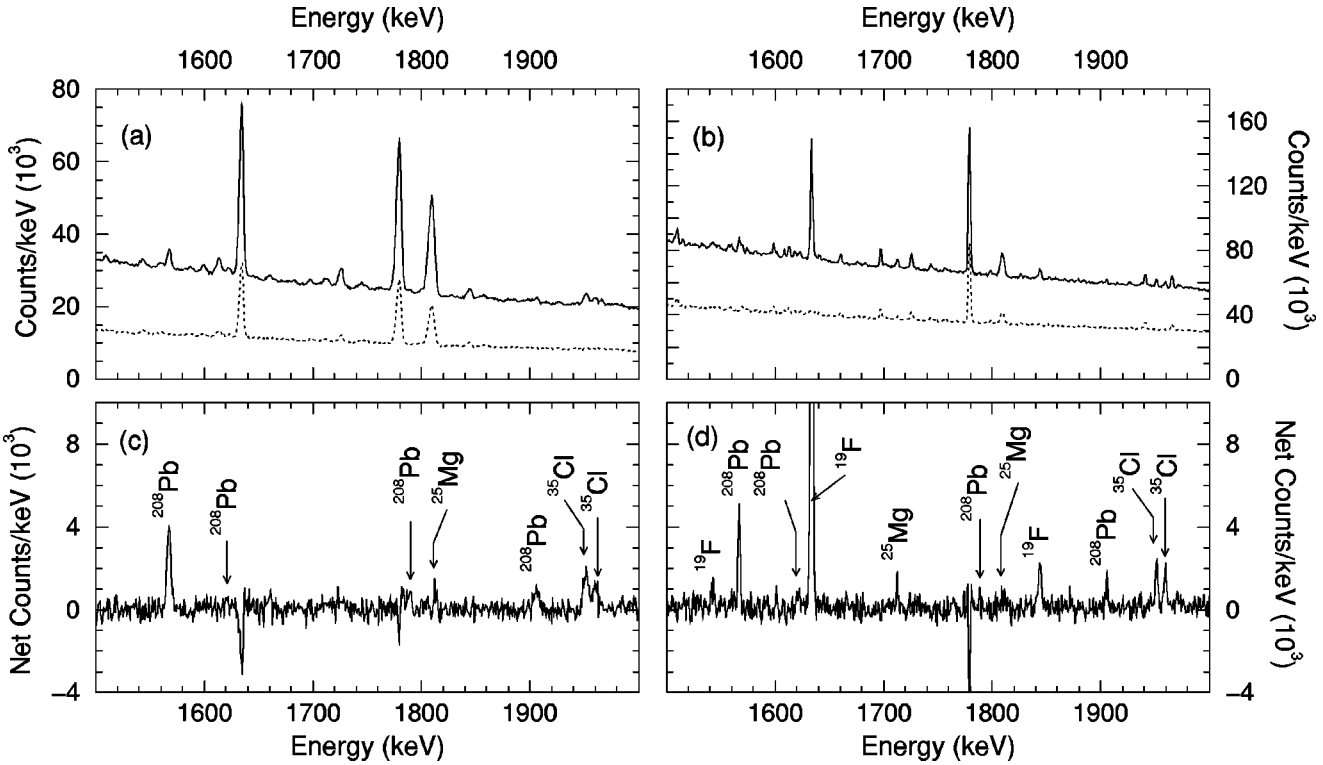

FIG. 1. (a) γ-ray energy spectra collected using the composite sample of radiogenic lead and reactor-grade graphite (solid line) and using the graphite sample only (dashed line) are shown. The spectrum collected using the graphite has been multiplied by an arbitrary normalization. (b) γ-ray energy spectra collected using the radiogenic lead sample (solid line) and with no sample in place (dashed line) are shown. The background spectrum collected with no sample has been multiplied by an arbitrary normalization. (c) The net spectrum obtained by subtracting the spectrum taken with the graphite sample from the spectrum taken with the composite sample [normalized to the ^{12}C$(n,\gamma)^{13}$C reaction] is shown. The origins of the most prominent lines are indicated. (d) The net spectrum obtained by subtracting the spectrum taken with no sample from the spectrum taken with the radiogenic lead sample (normalized by the ratio of the collection times) is shown.

where $\epsilon(E_\gamma)$ is the photopeak efficiency of the detector for detecting a γ ray of energy E_γ, and 4.11 is the ratio of ^{12}C to ^{208}Pb atoms in the composite sample. The ^{208}Pb$(n,\gamma)^{209}$Pb cross sections were also normalized to the 3684-keV γ ray from the ^{12}C$(n,\gamma)^{13}$C reaction in a similar manner.

TABLE II. The cross sections for production of γ rays from the ^{208}Pb$(n,\gamma)^{209}$Pb reaction with thermal neutrons.

E_γ (keV)[b]	PbC sample I_γ (μb)[b]	Pb sample[a] I_γ (μb)[b]	Adopted I_γ(μb)[b]	Placement
465.3 (3)	188 (17)	166 (14)	175 (12)	2032→1567
970.5 (5)	21 (9)	25 (10)	23 (7)	2538→1567
1400.3 (3)	21(4)	[42 (10)][c]	25 (5)	C→2538
1567.1 (3)	230 (12)		230 (12)	1567→0
1621.5 (7)	21 (13)	34 (12)	28 (9)	C→2319
1788.3 (4)	54 (11)	42 (15)	51 (9)	C→2149
1905.7 (4)	78 (13)	79 (14)	78 (10)	C→2032

[a]The cross sections were determined relative to the 1567-keV γ ray.
[b]In this notation 465.3 (3)≡465.3±0.3, 188 (17)≡188±17, etc. The uncertainties refer to one standard deviation.
[c]Contaminated by neutron capture on the cadmium between the sample and detector.

We assume that the ratios of the ^{208}Pb$(n,\gamma)^{209}$Pb cross sections to the ^{12}C$(n,\gamma)^{13}$C cross sections at the cold neutron energies used in our measurement are the same as the ratios at thermal energies. Therefore, the *thermal* cross sections for the ^{208}Pb$(n,\gamma)^{209}$Pb reaction were determined from Eq. (3.1) by setting the ^{12}C$(n,\gamma)^{13}$C cross sections to the measured values using a thermal-neutron beam, $I_{1262}=1.09\pm0.02$ mb and $I_{3684}=1.08\pm0.02$ mb [31]. The cross sections obtained using these two γ rays for normalization were consistent within statistical uncertainty, and the average of the two values is provided in the second column of Table II. The uncertainties in the relative γ-ray efficiencies (2–3 %) and in the ^{12}C capture cross sections (2%) have been added in quadrature to the statistical uncertainties to arrive at the uncertainties given in Table II, but these are insignificant compared to the statistical uncertainties except for the strongest γ ray. The uncertainty in the number of target atoms is negligible.

Several of the observed transitions are weak (less than 3σ observations), and additional measurements were performed to improve the sensitivity. The high-purity germanium detector in the PGAA spectrometer suffered some damage from neutron irradiation and was replaced with a detector with improved resolution. A thin piece of cadmium was added between the sample and the detector to reduce background from neutrons scattered from the sample.

TABLE III. Level scheme of ^{209}Pb as determined from this work.

E_x[a] (keV)	E_x (Ref. [32]) (keV)	J^π	Deexciting γ rays	ΣI_γ(in) (μb)	ΣI_γ(out) (μb)	ΣI_γ (in−out) (μb)
0.0	0.0	$\frac{9}{2}^+$		230 (12)		230 (12)
1567.1 (3)	1567.09 (3)	$\frac{5}{2}^+$	1567.1	198 (14)	230 (12)	−32(19)
2032.4 (4)	2032.22 (4)	$\frac{1}{2}^+$	465.3	157 (17)	175 (12)	−18(21)
2149.7 (7)	2149.43 (4)	$\frac{1}{2}^-$	117[b]	51 (9)	51 (9)	0 (13)
2316.5 (9)	2319 (2)	$(\frac{3}{2}^-)$	284[b]	28 (9)	28 (9)	0 (13)
2537.7 (5)	2538 (2)	$\frac{3}{2}^+$	970.5	25 (5)	23 (7)	2 (9)
3938.0 (5)	3936.8 (1.4)	$\frac{1}{2}^+$	1400.3, 1621.5, 1788.3, 1905.7		182 (17)	−182(17)

[a]In this notation 1567.1 (3)≡1567.1±0.3.

[b]Unobserved because of the large background at low γ-ray energies. The intensity is inferred from the known decay scheme [32].

A portion of a γ-ray energy spectrum collected for 109.5 h using the radiogenic lead sample is shown in Fig. 1(b). A background spectrum was also collected with no sample in place. The background spectrum, divided by an arbitrary normalization, is also shown in Fig. 1(b). The background spectrum was normalized to the spectrum collected using the radiogenic lead sample by the ratio of the collection times and subtracted from the lead spectrum. The same energy region of this background-subtracted spectrum is shown in Fig. 1(d). No additional γ rays from the ^{208}Pb$(n,\gamma)^{209}$Pb reaction were observed in this measurement. The cross sections for the ^{208}Pb$(n,\gamma)^{209}$Pb reaction are given in column 3 of Table II, where the cross sections have been normalized to that of strongest γ ray, the 1567-keV ground-state transition. The yields of all of the observed transitions agree with those of the previous measurement except for the peak at 1400 keV, which was contaminated by a background peak arising from the capture of scattered neutrons by the cadmium placed between the sample and the detector. We adopt a weighted average of the values from the two measurements which is shown in column 4 of Table II.

IV. PLACEMENT OF THE OBSERVED TRANSITIONS IN ^{209}Pb

The placement of the seven observed γ rays in the ^{209}Pb level scheme is summarized in the last column of Table II. The energies of three of the observed γ rays correspond to previously reported transitions among known levels in ^{209}Pb [32]. These are $E_\gamma = 1567.1 \pm 0.3$ keV, corresponding to the ground-state transition from the $\frac{5}{2}^+$ level at $E_x = 1567$ keV; $E_\gamma = 465.3 \pm 0.3$ keV, the transition from the $\frac{1}{2}^+$ level at $E_x = 2032$ keV to the $\frac{5}{2}^+$ level at $E_x = 1567$ keV; $E_\gamma = 970.5 \pm 0.5$ keV, the transition from the $\frac{3}{2}^+$ level at $E_x = 2538$ keV also populating the $\frac{5}{2}^+$ level at $E_x = 1567$ keV. The other four observed γ rays, $E_\gamma = 1400.3 \pm 0.3$, 1621.5 ± 0.7, 1788.3 ± 0.4, and 1905.7 ± 0.4 keV, were identified as primary transitions from the capturing state to excited states in ^{209}Pb at $E_x = 2538$, 2319, 2149, and 2032 keV, respectively.

The level scheme of ^{209}Pb deduced from our work is summarized in Table III. The energies determined from each level are consistent with the adopted value from the literature [32]; however, we have obtained more precise energies for the levels at 2316.5 ± 0.9 and 2537.7 ± 0.5 keV. In addition, we determined the neutron-separation energy (S_n) of ^{209}Pb to be 3938.0 ± 0.5 keV. Our placements are also summarized in Fig. 2.

We have established a nearly complete picture of the neutron capture spectrum of ^{208}Pb. The observed cross section populating each level, ΣI_γ(in), and the observed cross section from the deexcitation of each level, ΣI_γ(out), are shown in the fifth and sixth columns of Table III. If the level scheme

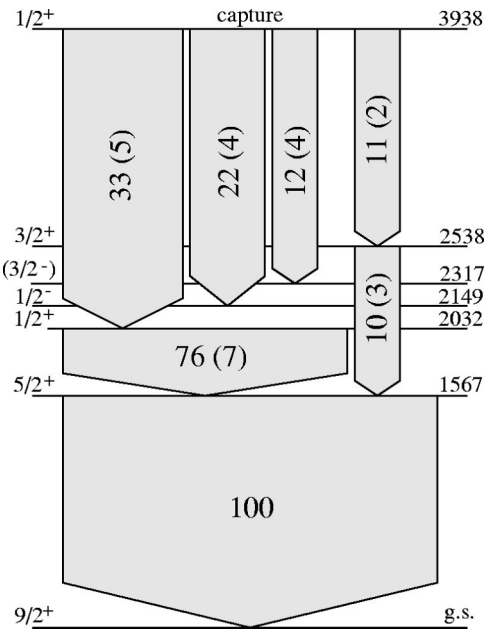

FIG. 2. A partial level scheme of ^{209}Pb is shown. The observed γ rays from the ^{208}Pb$(n,\gamma)^{209}$Pb reaction are indicated. The widths of the lines (and the included numbers) show the relative strengths of the transitions normalized to the 1567-keV ground-state transition.

TABLE IV. The measured total capture cross sections for the lead isotopes are compared to the values determined from previous measurements.

Isotope	Cross section (mb)	Reference	This work (mb)
^{204}Pb	661±70	Ref. [38]	–
^{206}Pb	30.5±0.7	Refs. [35,36]	26.6±1.2
^{207}Pb	709±10	Refs. [35,36]	610±30
^{208}Pb	0.487±0.030	Ref. [24]	0.230±0.012
Natural Pb	171±2	Ref. [36]	(151±7)[a]

[a]The cross section for neutron capture by ^{204}Pb was taken to be 661±70 mb from Jurney, Motz, and Vegors [38].

is complete, the observed cross sections populating and depopulating each level should be equal. The 117- and 284-keV γ rays from the decays of the 2149- and 2317-keV levels to the 2032-keV level were not observed because of the large background at low γ ray energies, but we infer the strengths of these transitions from the known decay branchings of these levels [32]. Given the inferred strengths of these two low-energy γ rays, ΣI_γ(in) is generally well balanced by ΣI_γ(out). A small missing contribution, $I_\gamma \approx 30$ μb, capturing into levels with $E_x > 2032$ and cascading through the $E_x = 1567$ keV level, i.e., $C \rightarrow E_x \rightarrow 1567 \rightarrow 0$, would balance the intensities for all observed levels, including the intensities of the primary and ground-state transitions. This small remaining strength could be fractionated, making it too weak to be observed in these measurements.

The experimental spectra were carefully studied for other possible primary and ground-state transitions. None were found exceeding the experimental sensitivity of about 10 μb. We conclude that all of the capture strength cascades through the $E_x = 1567$ keV ($\frac{5}{2}^+$) state, and that the total thermal cross section for the ^{208}Pb$(n,\gamma)^{209}$Pb reaction is essentially equal to the cross section for production of the 1567-keV γ ray, i.e., $\sigma_{208} = 230 \pm 12$ μb.

V. OTHER LEAD ISOTOPES

The 6739- and 7368-keV γ rays from neutron capture on ^{206}Pb and ^{207}Pb were also observed in these measurements. From our work and from previous measurements [33,34] it can be shown that these transitions represent greater than 99% of the capture by these isotopes. A direct measurement of the capture cross section for these transitions has not been previously reported. The ratio of these cross sections (I_{6739}/I_{7368}) was previously measured to be 0.043±0.001 by Jurney and Motz [35]. We find $(I_{6739}/I_{7368}) = 0.0435 \pm 0.0013$, in good agreement with the previous measurement. Normalizing the yields of the 6739- and 7368-keV γ rays to those from the ^{12}C$(n,\gamma)^{13}$C reaction, we also find $I_{6739} = 26.3 \pm 1.2$ mb and $I_{7368} = 600 \pm 30$ mb. The previously reported values for the ^{206}Pb and ^{207}Pb neutron capture cross sections were determined from a measurement of the cross section for neutron absorption on natural lead using a pile oscillator [36] and from the measured ratios of the ^{204}Pb and ^{206}Pb cross sections to that of ^{207}Pb [35]. [The ^{208}Pb$(n,\gamma)^{209}$Pb cross section was taken to be negligible.] Our cross sections for ^{206}Pb and ^{207}Pb are compared to the previous values in Table IV and are found to be about 13% lower. The source of this discrepancy is not known; however, the total capture cross section for many elements (magnesium [10] and copper [37], for example) has been found to be about 7% lower than determined by the pile oscillator measurements of Ref. [36]. This could explain much of the observed discrepancy.

VI. THEORETICAL CONSIDERATIONS

Because ^{208}Pb is a double closed-shell nucleus, it is possible to calculate neutron capture cross sections with reasonable accuracy. Two contributions need to be considered. The first is the compound-nuclear contribution, governed by a nearby resonance or bound state. The second is direct capture.

Two consequences of the shell nature of ^{208}Pb are that the neutron separation energy of the compound nucleus ^{209}Pb is low, only 3.938 MeV, and so is the level density. Thus, it is believed that most of the levels below the neutron separation energy are known. Certainly, there is not an order of magnitude change in the level spacing of the $J^\pi = \frac{1}{2}^-$ and $\frac{3}{2}^-$ levels between those found in reactions such as (d,p) below the neutron separation energy and those found by the much higher resolution technique of neutron cross-section measurements above that energy.

There is only one known $\frac{1}{2}^+$ level below the neutron separation energy. This level is at 2.032 MeV, and it has a (d,p) spectroscopic factor of 0.98. Thus, we identify it as the $4s_{1/2}$ single-particle neutron level. The next known $\frac{1}{2}^+$ level is the *s*-wave resonance at 0.507 MeV. This resonance has a neutron width of 53 keV, giving a reduced width that is 3% of a nominal single-particle value. Because the sensitivity of the (d,p) work done on this nucleus is such that levels with spectroscopic factors of the order of 0.001 have been detected, it is unlikely that there are any other bound $\frac{1}{2}^+$ levels approaching the neutron strength of the 0.507-MeV resonance apart from the 2.032-MeV state. Being a nearly pure single-particle state, the latter will have its main effect on the thermal-neutron cross sections through its effect on the neutron scattering length and hence on the direct-capture cross section. It follows that the only state we need to consider in computing the magnitude of the compound-nuclear capture is the 0.507-MeV resonance. (The next *s*-wave resonance is at 1.735 MeV and has a similar reduced neutron width).

We show in column 5 of Table V the expected values of the thermal-neutron capture cross sections from the 0.507-MeV resonance state to the known $\frac{1}{2}^-$ and $\frac{3}{2}^-$ bound states of ^{209}Pb. The model for the $E1$ transition strength is the Weisskopf estimate modified by using a sampling of realistic calculations of the radial dipole integrals [39]. The formula for the radiation width is

$$\Gamma_\gamma = 2.5 \times 10^{-9} E_\gamma^3 A^{1/2} D, \tag{6.1}$$

TABLE V. Properties of all $J=\frac{1}{2}$ or $\frac{3}{2}$ states in ^{209}Pb below the neutron threshold, including both the measured and calculated [compound-nuclear (CN) and direct] cross sections for thermal-neutron capture to these states.

E_x (keV)	J^π	S	E_γ (keV)	CN I_γ (μb)	Direct I_γ (μb)	Measured I_γ (μb)
2032	$\frac{1}{2}^+$	0.98 ($4s_{1/2}$)	1904	(59) [a]	66	78±10
2149	$\frac{1}{2}^-$	0.0036 (if $4p_{1/2}$)	1787	240	62	51±9
2319	$(\frac{3}{2}^-)$	0.0045 (if $4p_{3/2}$)	1617	180	151	28±9
2538	$\frac{3}{2}^+$	1.09 ($3d_{3/2}$)	1398	(23) [a]	0	25±4
2904	$\frac{3}{2}^-$		1032	47		<10
3031	$(\frac{1}{2}^-,\frac{3}{2}^-)$	0.0012 (if $4p_{3/2}$)	905	31	32	<14
3076	$\frac{3}{2}^-$		860	27		<10
3524	$\frac{3}{2}^-$		412	3		
3562	$\frac{3}{2}^-$		374	2		
3637	$\frac{3}{2}^-$		299	1		
3681	$(\frac{1}{2}^-,\frac{3}{2}^-)$	0.0029 (if $4p_{1/2}$)	255	1	15	
3831	$\frac{3}{2}^-$		105			

[a]This is unlikely to be a typical compound-nuclear transition (see text) and is therefore not included in the total cross section for the contribution from the compound-nuclear mechanism.

where E_γ is the energy of the transition in MeV, A is the nuclear mass number and D is the initial state level spacing, for which we have used the value of ~1 MeV. Only a few transitions contribute to the expected total compound-nuclear capture cross section of 0.53 mb. Because the individual transition cross sections are subject to Porter-Thomas fluctuations, there is a large variance associated with this expectation value. The distribution of likely total cross-section values about the expectation value will be approximately exponential, giving only about one-third chance for the actual cross section being greater than the expectation value. A widely used empirical version of the Weisskopf model is Cameron's formula [40]:

$$\Gamma_\gamma = 0.33\times 10^{-9} E_\gamma^3 A^{1/2} D. \tag{6.2}$$

This formula gives cross-section estimates about 40% of those given by Eq. (6.1).

Another important experimental observation is that $M1$ transitions in resonance neutron capture are, on average, about one fifth of the strength of the $E1$ transitions. On this basis, the transitions to the two even-parity states at 2.032 MeV and 2.538 MeV will contribute an expected additional 15% to the total capture cross section. These are both almost pure single-particle states, however, and this fact should greatly reduce the transition strength, the typical compound-nuclear component going only to the small residue of the final state that is not of single-particle character. This aspect is considered further in the next paragraph.

Thermal-neutron direct capture [4] has been shown quantitatively through a series of papers [6–10] to be the preponderant mechanism for $E1$ transitions over a broad range of light nuclei. Only a few nuclei with strong resonances fairly close to thermal-neutron energy are exceptions to this rule. Nuclei that are near to closed shells are also expected to be candidates for exhibiting the direct mechanism, because they too are likely to have final states with strong single-particle admixtures. In the case of ^{209}Pb, however, the $3p_{1/2}$ and $3p_{3/2}$ neutron states are already occupied with the shell closure of ^{208}Pb, and the $4p$ states are expected to lie much higher in the continuum. In the spectrum below the neutron separation energy, there are several $\frac{1}{2}^-$ and $\frac{3}{2}^-$ states, as shown in Table V, but their spectroscopic factors are considerably less than 1%. These states could be small residues from the $3p$ states or weak fragments well out on the lower wings of the fractionated $4p$ states. However, if these single-particle strengths are used to evaluate the direct-capture cross sections with the method described in Ref. [41], the results shown in column 5 of Table V are obtained, giving a total $E1$ direct-capture cross section of 0.26 mb. The spectroscopic factors are not available for several states; presumably they are too small to be measured reliably, and we therefore assume the corresponding direct-capture cross sections to be negligible. The direct-capture components can interfere constructively or destructively with the compound-nuclear (CN) components, but on average the two sets should be added. Using the CN cross sections given in Table V, we obtain a total capture cross section of 0.79 mb, or 0.47 mb if the Cameron model is used for the CN component. The measured cross sections for individual transitions differ at most by an order of magnitude from the estimated CN strengths, and these differences are not inconsistent with the expected Porter-Thomas fluctuations in the individual strengths.

Direct $M1$ capture is very weak; convincing evidence of it has only been found in a few very light nuclei [42]. The

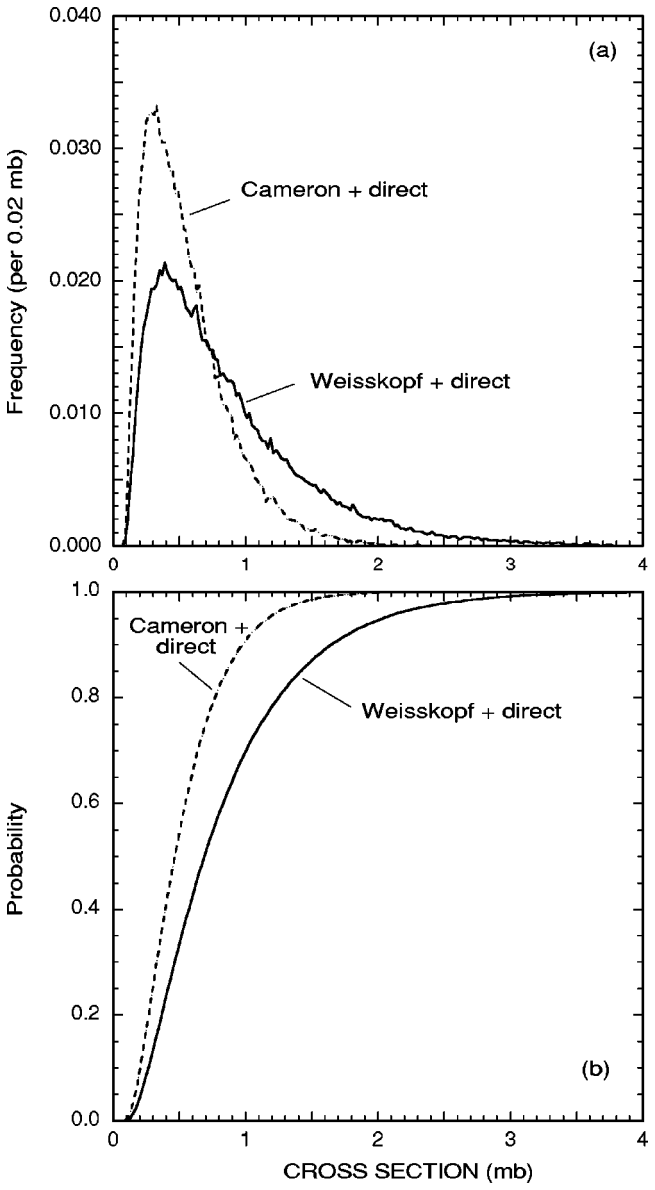

FIG. 3. (a) Frequency functions for the total capture cross section of ^{208}Pb calculated by combining direct capture with either the modified Weisskopf or Cameron model of compound-nuclear capture are shown. (b) The probability distributions for the total capture cross section of ^{208}Pb are shown.

single-particle nature of the two final states to which $M1$ transitions are allowed suggests, however, that it should be considered. Direct capture to the 2.538-MeV $\frac{3}{2}^+$ state is ruled out by its single-particle $d_{3/2}$ character. The direct-capture cross section to the 2.032-MeV $\frac{1}{2}^+$ state (single-particle character $4s_{1/2}$) is calculated to be 0.066 mb. This value is about the same, as would be estimated from the CN model, ignoring the single-particle character of the final state. It can be concluded, therefore, that $M1$ transitions contribute no more than 10–15 % to the ^{208}Pb capture cross section.

To make an assessment of the degree to which theory is in agreement with experiment, it is necessary to know the probability distribution of the theoretical estimates. In Table V

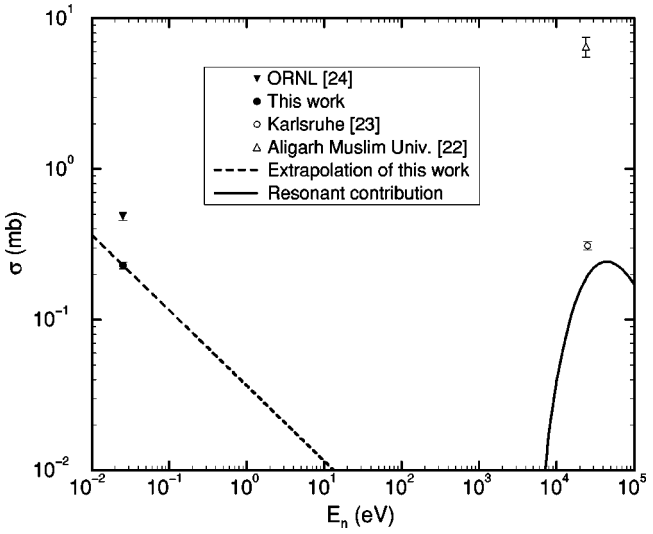

FIG. 4. The three previously reported measurements of the total ^{208}Pb$(n,\gamma)^{209}$Pb cross section are shown with the results of this measurement.

the direct-capture estimates are precise, whereas the compound-nuclear components will have Porter-Thomas distributions. So even for a single transition, the analytical form of the frequency function is quite complicated, ranging from a narrow Gaussian when $\sigma_{\mathrm{CN}(\gamma)} \ll \sigma_{\mathrm{dir}(\gamma)}$ to a Porter-Thomas form at the opposite extreme. For the convolution of the several transitions in Table V, we have resorted to a Monte Carlo numerical method. The total capture cross section has the form

$$\sigma_i = \sum_i \left(\sigma_{i(\mathrm{CN})}^{1/2} + \sigma_{i(\mathrm{dir})}^{1/2}\right)^2. \tag{6.3}$$

The values of the direct components are the square roots of the entries in Table V and are taken to have positive definite sign. The CN components are drawn from a Gaussian distribution with zero mean and dispersion equal to $\sqrt{(2\langle\sigma_{i(\mathrm{CN})}\rangle)}$. The resulting frequency function and probability distribution for the values given in Table V are shown in Fig. 3. The mean value is 0.86 mb and the variance is 0.36 mb^2. The frequency function and probability distribution for the Cameron model of CN capture are also shown in Fig. 3. The mean value is 0.55 mb and the variance is 0.10 mb^2.

The measured value of the cross section is 0.230 ± 0.012 mb. The probability of the cross section being 0.230 mb or less on the modified Weisskopf model is 6.8%. On the Cameron model it is about 14%. With the expected compound-nuclear contribution being an order of magnitude less than that used for the modified Weisskopf model above, the probability is only about 13%. These probabilities are sufficiently high to suggest that the model of CN capture interfering with a smaller but still significant component of direct capture is a reasonable one.

VII. CONCLUSION

We have measured the thermal-neutron capture cross sections for the ^{206}Pb, ^{207}Pb, and ^{208}Pb isotopes. Seven γ rays

from the ^{208}Pb$(n,\gamma)^{209}$Pb reaction were observed, and a level scheme in ^{209}Pb was constructed which establishes a nearly complete picture of the capture spectrum. The thermal-neutron capture cross section for ^{208}Pb was found to be 0.230 ± 0.012 mb. Our result is plotted in Fig. 4 with the other reported measurements of the total ^{208}Pb$(n,\gamma)^{209}$Pb cross section. We find the thermal-neutron capture cross section to be about a factor of 2 smaller than reported by Emery [24]. The source of this discrepancy is not clear.

The ^{208}Pb$(n,\gamma)^{209}$Pb cross section extrapolated as a function of energy from our measurement is shown in Fig. 4 (dashed line). This extrapolation is accurate for low neutron energies, where the centrifugal barrier restricts capture to only *s*-wave neutrons. In the energy region that is important for the *s* process, $E_n = 5 - 30$ keV, resonances and capture of *p*-wave neutrons can contribute significantly to the cross section. Also shown in Fig. 4 is the Maxwellian-averaged cross section resulting from known resonances (solid line) [16]. The known resonances and the *s*-wave contribution to the cross section do not account for the reported total cross sections at 25 keV. The differing flux distributions of incident neutrons might be a reason why the two measured values near 25 keV (see Fig. 4) are widely discrepant because of strong resonances at $E_n > 40$ keV. It has been proposed [16] that a *p*-wave direct-capture contribution could account for the difference between the cross section due to known resonances and the total cross section measurement of Ratzel [23]. A measurement of the ^{208}Pb$(n,\gamma)^{209}$Pb capture cross section and energy spectrum at neutron energies around 1 to 10 keV, where both the *s*-wave and resonant contributions to the cross section are expected to be small, would be particularly desirable to test calculations of this *p*-wave component and to reduce the uncertainty that remains in the cross section in the energy region that is important for the *s* process.

ACKNOWLEDGMENTS

Oak Ridge National Laboratory is managed by UT-Battelle, LLC, for the U.S. Department of Energy under Contract No. DE-AC05-00OR22725. The Joint Institute for Heavy Ion Research has as member institutions the University of Tennessee, Vanderbilt University, and the Oak Ridge National Laboratory; it is supported by the members and by the U.S. Department of Energy under Contract No. DE-FG05-87ER40361. Los Alamos National Laboratory is managed by the University of California for the U.S. Department of Energy under Contract No. W-7405-ENG-36.

[1] N.E. Holden, in *CRC Handbook of Chemistry and Physics*, edited by D.R. Lide (CRC Press, Boca Raton, 1999), p. 159.
[2] G. Audi and A.H. Wapstra, Nucl. Phys. **A595**, 409 (1995).
[3] S.I. Sukhoruchkin, Z.N. Soroko, and V.V. Deriglazov, in *Tables of Neutron Resonance Parameters*, edited by H. Schopper, Landolt-Börnstein, New Series, Group I, Vol. 16, Pt. B (Springer, Berlin, 1989), p. 414.
[4] A.M. Lane and J.E. Lynn, Nucl. Phys. **17**, 563 (1960); **17**, 586 (1960).
[5] A. Mengoni, T. Otsuka, T. Nakamura, and M. Ishihara, Nucl. Phys. **A621**, 323c (1997).
[6] E.T. Jurney, J.W. Starner, J.E. Lynn, and S. Raman, Phys. Rev. C **56**, 118 (1997).
[7] S. Raman, E.K. Warburton, J.W. Starner, E.T. Jurney, J.E. Lynn, P. Tikkanen, and J. Keinonen, Phys. Rev. C **53**, 616 (1996).
[8] M.C. Moxon, J.A. Harvey, S. Raman, J.E. Lynn, and W. Ratynski, Phys. Rev. C **48**, 553 (1993).
[9] S. Raman, E.T. Jurney, J.W. Starner, and J.E. Lynn, Phys. Rev. C **46**, 972 (1992).
[10] T.A. Walkiewicz, S. Raman, E.T. Jurney, J.W. Starner, and J.E. Lynn, Phys. Rev. C **45**, 1597 (1992).
[11] J.E. Lynn, E.T. Jurney, and S. Raman, Phys. Rev. C **44**, 764 (1991).
[12] S. Raman, R.F. Carlton, J.C. Wells, E.T. Jurney, and J.E. Lynn, Phys. Rev. C **32**, 18 (1985).
[13] B.S. Meyer, Annu. Rev. Astron. Astrophys. **32**, 153 (1994).
[14] J.J. Cowan, B. Pfeiffer, K.-L. Kratz, F.-K. Thielemann, C. Sneden, S. Burles, D. Tytler, and T.C. Beers, Astrophys. J. **521**, 194 (1999).
[15] H. Beer, Astrophys. J. **379**, 409 (1991).
[16] H. Beer, F. Corvi, and P. Mutti, Astrophys. J. **474**, 843 (1997).
[17] R.L. Macklin, J. Halperin, and R.R. Winters, Astrophys. J. **217**, 222 (1977).
[18] B.J. Allen, R.L. Macklin, R.R. Winters, and C.Y. Fu, Phys. Rev. C **8**, 1504 (1973).
[19] D.G. Kovar, N. Stein, and C.K. Bockelman, Nucl. Phys. **A231**, 266 (1974).
[20] E.R. Flynn, G. Igo, P.D. Barnes, D. Kovar, D. Bes, and R. Broglia, Phys. Rev. C **3**, 2371 (1971).
[21] T. Rauscher, R. Bieber, H. Oberhummer, K.-L. Kratz, J. Dobaczewski, P. Möller, and M.M. Sharma, Phys. Rev. C **57**, 2031 (1998).
[22] A.K. Chaubey and M.L. Sehgal, Phys. Rev. **152**, 1055 (1966).
[23] U. Ratzel, Diplomarbeit, Universität Karlsruhe (1988).
[24] J.F. Emery, Oak Ridge National Laboratory Report No. ORNL-4343 (1971), p. 71.
[25] R.M. Lindstrom, J. Res. Natl. Inst. Stand. Technol. **98**, 127 (1993).
[26] R.L. Paul, R.M. Lindstrom, and A.E. Heald, J. Radioanal. Nucl. Chem. **215**, 63 (1997).
[27] *X-Ray and Gamma-Ray Standards for Detector Calibration*, IAEA-TECDOC-619 (International Atomic Energy Agency, Vienna, 1991).
[28] S. Raman, C. Yonezawa, H. Matsue, H. Iimura, and N. Shinohara, Nucl. Instrum. Methods Phys. Res. A **A454**, 389 (2000).
[29] M.A. Lone, R.A. Levitt, and D.A. Harrison, At. Data Nucl. Data Tables **26**, 511 (1981).

[30] R.C. Reedy and S.C. Frankle, At. Data Nucl. Data Tables **80**, 1 (2001).
[31] E.T. Jurney, P.J. Bendt, and J.C. Browne, Phys. Rev. C **25**, 2810 (1982).
[32] M.J. Martin, Nucl. Data Sheets **63**, 723 (1991).
[33] P. Hungerford, T. von Egidy, H.H. Schmidt, S.A. Kerr, H.G. Börner, and E. Monnand, Z. Phys. A **313**, 349 (1983).
[34] M.A.J. Mariscotti, D.R. Bes, S.L. Reich, H.M. Sofía, P. Hungerford, S.A. Kerr, K. Schreckenbach, and W.F. Davidson, Nucl. Phys. **A407**, 98 (1983).
[35] E.T. Jurney and H.T. Motz, Argonne National Laboratory Report No. ANL-6797, 236 (1963).
[36] D. Jowitt, S.K. Pattenden, H. Rose, V.G. Small, and R.B. Tattersall, United Kingdom Atomic Energy Research Establishment Report No. AERE R/R 2516 (1959).
[37] W. Dilg and W. Mannhart, Z. Phys. **266**, 157 (1974).
[38] E.T. Jurney, H.T. Motz, and S.H. Vegors, Jr., Nucl. Phys. **A94**, 351 (1967).
[39] J.E. Lynn, *Theory of Neutron Resonance Reactions* (Oxford University Press, Oxford, 1968).
[40] A.G.W. Cameron, Can. J. Phys. **35**, 666 (1957).
[41] S. Kahane, J.E. Lynn, and S. Raman, Phys. Rev. C **36**, 533 (1987).
[42] S. Raman, S. Kahane, and J.E. Lynn, in *Proceedings of the International Conference on Nuclear Data for Science and Technology, Mito, Japan, 1988*, edited by S. Igarasi (Saikon, Tokyo, 1988), p. 645.